

The authors have addressed most of raised comments in the revised manuscript with comprehensive explanations in the replies. I would still like to raise several minor issues and hope they would be helpful for the further improvement of the manuscript.

We would like to thank the reviewer for her/his positive evaluation and the very helpful comments and suggestions. Below we reply on each specific comment.

1. The authors add a section to demonstrate the uncertainties of flux estimation which could be as high as 30%. Please quantitatively clarify if such high uncertainty would invalidate the model estimation since I don't see the model sensitivity analysis in the manuscript.

Reply: As the uncertainties of the flux estimation are unbiased (i.e. they vary randomly), they do not change the general results of the model. We added this explanation to the uncertainty analysis.

2. In Table 3, the authors compile a large dataset of carbon export of World Rivers for the purpose of comparison with present study. For the Amazon River, Richey et al. (2002) estimated the CO₂ evasion of 1.2 Mg C ha⁻¹ yr⁻¹, which was around 87% of total aquatic carbon export. This is different from the value cited in Table 3 (78 g C m⁻² yr⁻¹). Probably I am wrong here.

Reply: We changed the value to 138 g C m⁻² yr⁻¹.

3. The authors define the aquatic carbon export/NPP ratio as the portion of terrestrial NPP exported by rivers (See P6 Line 192) and frequently make similar statements based on the definition in the sections of Abstract, Discussions and Conclusion. While the NPP and NEP are the main controlling factors regulating the aquatic carbon export, the export/NPP ratio doesn't directly mean that the certain fraction of NPP is exported by rivers. Instead, it only indicates the aquatic carbon export flux represents certain amount of NPP.

Reply: We changed the definition in line 192 to "the ratio of the carbon exported through the aquatic network (i.e. the sum of evasion and discharge) to the terrestrial NPP" and the statements in Abstract, Discussion and Conclusion to "13.9 g C m⁻² yr⁻¹, corresponding to 2.7 % of terrestrial NPP".

4. While this study presents a representative investigation of temperate watersheds, which are a critical component of terrestrial ecosystems and carbon cycling. I would suggest the authors to address the implications of this study in a broad background of global carbon cycling and to clearly unravel their contributions to improve the understanding of the roles of temperate inland water bodies in the regional and global carbon cycles.

Reply: We added the following sentence to the Introduction: "In this study, we provide a representative investigation of a temperate watershed to improve the understanding of the role of temperate inland water bodies in the regional and global carbon cycles."

1 Regional-scale lateral carbon transport and CO₂ evasion in 2 temperate stream catchments

3

4 Katrin Magin¹, Celia Somlai-Haase¹, Ralf B. Schäfer¹ and Andreas Lorke¹

5 ¹Institute for Environmental Sciences, University of Koblenz-Landau, Fortstr. 7, D-76829 Landau, Germany

6 *Correspondence to:* Katrin Magin (magi6618@uni-landau.de)

7

8

9 **Abstract.** Inland waters play an important role in regional to global scale carbon cycling by transporting, processing
10 and emitting substantial amounts of carbon, which originate mainly from their catchments. In this study, we
11 analyzed the relationship between terrestrial net primary production (NPP) and the rate at which carbon is exported
12 from the catchments in a temperate stream network. The analysis included more than 200 catchment areas in
13 southwest Germany, ranging in size from 0.8 to 889 km² for which CO₂ evasion from stream surfaces and
14 downstream transport with stream discharge were estimated from water quality monitoring data, while NPP in the
15 catchments was obtained from a global data set based on remote sensing. We found that on average ~~2.7% of~~
16 ~~terrestrial NPP~~ (13.9 g C m⁻² yr⁻¹) (corresponding to 2.7% of terrestrial NPP) are exported from the catchments by
17 streams and rivers, in which both CO₂ evasion and downstream transport contributed about equally to this flux. The
18 average carbon fluxes in the catchments of the study area resembled global and large-scale zonal mean values in
19 many respects, including NPP, stream evasion as well as the carbon export per catchment area in the fluvial
20 network. A review of existing studies on aquatic-terrestrial coupling in the carbon cycle suggests that the carbon
21 export per catchment area varies in a relatively narrow range, despite a broad range of different spatial scales and
22 hydrological characteristics of the study regions.

23 **Keywords**

24 Regional carbon cycle, terrestrial-aquatic coupling, net primary production, CO₂ degassing from streams, land use

25 1 Introduction

26 Inland waters represent an important component of the global carbon cycle by transporting, storing and processing
27 significant amounts of organic and inorganic carbon (C) and by emitting substantial amounts of carbon dioxide
28 (CO₂) to the atmosphere (Cole et al., 2007;Aufdenkampe et al., 2011). Globally about 0.32 to 0.8 Pg C is emitted per
29 year as CO₂ from lakes and reservoirs (Raymond et al., 2013;Barros et al., 2011). For streams and rivers the global
30 estimates range from 0.35 to 1.8 Pg C yr⁻¹ (Raymond et al., 2013;Cole et al., 2007), where the lower estimates can
31 be considered as conservative because they omit CO₂ emissions from small headwater streams. In 2015 global CO₂
32 evasion from rivers and streams was estimated at 0.65 Pg C yr⁻¹ (Lauerwald et al., 2015). Comparable amounts of
33 carbon are discharged into the oceans by the world's rivers (0.9 Pg C yr⁻¹) and stored in aquatic sediments (0.6 Pg C
34 yr⁻¹) (Tranvik et al., 2009). In total, evasion, discharge and storage of C in inland waters have been estimated to
35 account for about 4 % of global terrestrial net primary production (NPP) (Raymond et al., 2013) or 50-70 % of the
36 total terrestrial net ecosystem production (NEP) (Cole et al., 2007). A recent continental-scale analysis, which
37 combined terrestrial productivity estimates from a suite of biogeochemical models with estimates of the total aquatic
38 C yield for the conterminous United States (Butman et al., 2015), resulted in mean C export rates from terrestrial
39 into freshwater systems of 4 % of NPP and 27 % of NEP. These estimates varied by a factor of four across 18
40 hydrological units with surface areas between 10⁵ and 10⁶ km².

41 The substantial lateral and vertical transport of terrestrial-derived C in inland waters is currently not accounted for in
42 most bottom-up estimates of the terrestrial uptake rate of atmospheric CO₂ (Battin et al., 2009) and results in high
43 uncertainties in regional-scale C budgets and predictions of their response to climate change, land use and water
44 management. Only few studies have quantified C fluxes and pools including inland waters at the regional-scale
45 ($O(10^3-10^4 \text{ km}^2)$) (Christensen et al., 2007;Buffam et al., 2011;Jonsson et al., 2007;Maberly et al., 2013) or for small
46 ($O(1-10 \text{ km}^2)$) catchments (Leach et al., 2016;Shibata et al., 2005;Billett et al., 2004). The majority of existing
47 regional-scale studies on terrestrial-aquatic C fluxes are from the boreal zone and are characterized by a relatively
48 large fractional surface area covered by inland waters, a high abundance of lakes and high fluvial loads of dissolved
49 organic carbon (DOC). Landscapes in the temperate zone can differ in all these aspects, potentially resulting in
50 differences in the relative importance of aquatic C-fluxes and flux paths (storage, evasion and discharge) in regional-
51 scale C budgets. In this study, we provide a representative investigation of a temperate watershed to improve the
52 understanding of the role of temperate inland water bodies in the regional and global carbon cycles. We ~~we~~ analyzed
53 the relationship between terrestrial NPP and CO₂ evasion and C discharge for more than 200 catchments in
54 southwest Germany. The stream-dominated catchments range in size from 0.8 to 889 km² and are characterized by a
55 relatively small fraction of surface water coverage (< 0.5 % of the land surface area). In contrast to studies from the
56 boreal zone, the fluvial C load is dominated by dissolved inorganic carbon (DIC). Estimates of aquatic C export
57 from the catchments were obtained from water quality and hydrological monitoring data and were related to
58 terrestrial NPP derived from MODIS satellite data. The scale dependence of aquatic carbon fluxes in relation to NPP
59 is analyzed by grouping the data according to Strahler stream order (Strahler, 1957). By comparing our results to a

60 variety of published studies, we finally discuss the magnitude as well as the relative importance of different fluvial
61 flux paths in regional-scale C budgets in different landscapes and climatic zones.

62 **2 Materials and Methods**

63 **2.1 Study area and hydrological characteristics**

64 The study area encompasses large parts of the federal state of Rhineland-Palatinate (RLP) in southwest Germany
65 (Fig. 1). The average altitude is 323 m (48 m - 803 m) and the mean annual temperature and precipitation varied
66 between 5.8 and 12.2 °C and 244 and 1576 mm during the time period between 1991 and 2011 at the 37
67 meteorological stations operated by the state RLP (<http://www.wetter.rlp.de/>). The dominating land cover in the
68 study area is woodland (41 %, mainly mixed and broad-leaved forest), tilled land (37 %, mainly arable land and
69 vineyards) and grassland (13 %, mainly pastures) (Corine land cover (EEA, 2006)). The fraction of peatland in the
70 study area is small (0.95 km²; 0.009% of the study area). 16 % of the study area contain carbonate bedrock.

71 Most of the rivers in RLP are part of the catchment area of the Rhine River. Other large rivers in the state are Mosel,
72 Lahn, Saar and Nahe. The upland regions of RLP are sources to many small, steep and highly turbulent streams with
73 gravel beds (MULEWF, 2015). Lakes in RLP are small with a total area of approximately 40 km² (Statistisches
74 Landesamt Rheinland-Pfalz, 2014) and were omitted from the analysis. The river network has a total length of
75 15800 km and consists of stream orders (Strahler, 1957) between 1 and 7. A catchment map of RLP, consisting of
76 subcatchments of 7729 river segments was provided by the state ministry (MULEWF, 2013), where a river segment
77 refers to the section between a source and the first junction with another river or between two junctions with other
78 rivers. All subsequent analyses were conducted separately for each stream order and streams of Strahler order >4
79 were omitted from the analysis because of the limited sample size with only few catchments available. Moreover,
80 we omitted streams for which parts of the catchment area were outside of the study area. Overall, 3377, 1619, 861
81 and 453 stream segments were retained for the analysis for Strahler order 1 to 4, respectively. Annual mean
82 discharge and length of the river segments were obtained from digital maps provided by the state ministry
83 (MULEWF, 2013).

84 **2.2 Aquatic carbon concentrations**

85 DIC concentrations and partial pressure of dissolved CO₂ (*p*CO₂) in stream water were estimated from governmental
86 water quality monitoring data which were acquired according to DIN EN ISO norms (DIN EN ISO 10523:2012-
87 04;DIN EN ISO 9963-1:1996-02;DIN EN ISO 9963-2:1996-02).. The data include measurements of alkalinity, pH
88 and temperature which were conducted between 1977 and 2011 (MULEWF, 2013). Sampling intervals differed
89 between the sites and water sampling was conducted irregularly with respect to year and season. To exclude a
90 potential bias resulting from the seasonality of DIC concentrations on the analysis, we only considered river
91 segments for which at least one measurement was available for each season (spring, summer, autumn, winter). From
92 these measurements, *p*CO₂ and DIC concentrations were estimated using chemical equilibrium calculations with the

93 software PHREEQC (Version 2) (Parkhurst and Appelo, 1999). For 201 river segments with seasonally resolved
 94 measurements, we first computed seasonal mean pCO_2 and DIC concentrations, which subsequently were aggregated
 95 to annual mean values averaged over the entire sampling period:

$$96 \overline{pCO_{2annual}} = (\overline{pCO_{2spring}} + \overline{pCO_{2summer}} + \overline{pCO_{2autumn}} + \overline{pCO_{2winter}})/4 \quad (1)$$

98 Measurements of dissolved and total organic C (DOC, TOC) were available only for 64 of these sampling sites.

99 2.3 Estimation of lateral DIC export and catchment-scale CO_2 evasion

100 The lateral export of DIC and the total CO_2 evasion from the upstream located stream network was calculated for
 101 each of the 201 sampling sites with seasonally averaged concentration estimates. Lateral DIC export from the
 102 corresponding catchments was calculated as the product of the mean DIC concentration and discharge. CO_2 evasion
 103 from the stream network upstream of each sampling site was estimated by interpolating pCO_2 for all river segments
 104 without direct measurements by averaging the mean concentrations by stream order and assigning them to all stream
 105 segments of the river network (Butman and Raymond, 2011). Stream width (w , in m), depth (d , in m) and flow
 106 velocity (v , in $m\ s^{-1}$) were estimated from the discharge (Q , in $m^3\ s^{-1}$) using the following empirical equations
 107 (Leopold and Maddock Jr, 1953):

$$108 w = a * Q^b \quad d = c * Q^d \quad v = e * Q^f, \quad (2)$$

109 For the hydraulic geometry exponents and coefficients, the values from Raymond et al. (2012) were used ($b=0.42$,
 110 $d=0.29$, $f=0.29$, $a=12.88$, $c=0.4$ and $e=0.19$).

111 The water surface area (A , in m^2) was calculated as the product of length and width of the river segments. The
 112 average slope for each segment was estimated from a Digital Elevation Map (resolution 10 m) provided by the
 113 federal state of Rhineland-Palatinate (LVermGeoRP, 2012). Zhang and Montgomery (1994) investigated the effect
 114 of digital elevation model (DEM) resolution on slope calculation and performance in hydrological models for spatial
 115 resolutions between 2 and 90 m. They found that while a 10-m grid is a significant improvement over 30 m or
 116 coarser grid sizes, finer grid sizes provide relatively little additional resolution. Thus a 10-m grid size represents a
 117 reasonable tradeoff between increasing spatial resolution and data handling requirements for modeling surface
 118 processes in many landscapes. The gas transfer velocity of CO_2 at $20^\circ C$ (k_{600} , in $m\ d^{-1}$) was calculated from slope (S)
 119 and flow velocity (v , in $m\ s^{-1}$) (Raymond et al., 2012).

$$120 k_{600} = S * v * 2841.6 + 2.03 \quad (3)$$

121 This gas transfer velocity was adjusted to the in situ temperature (k_T , in $m\ d^{-1}$) using the following equation:

$$122 k_T = k_{600} * \left(\frac{Sc_T}{600}\right)^{-0.5}, \quad (4)$$

123 where Sc_T is the Schmidt number (ratio of the kinematic viscosity of water and the diffusion coefficient of dissolved
 124 CO_2) at the in situ temperature (Raymond et al., 2012). Finally the CO_2 flux (F_D , in $g\ C\ m^{-2}\ yr^{-1}$) for each stream
 125 segment was calculated as:

$$126 F_D = k_T * K_H(pCO_2 - pCO_{2,a}) * M_C \quad (5)$$

127 The partial pressure of CO₂ in the atmosphere ($p\text{CO}_{2,a}$) was considered as constant (390 ppm) and the Henry
128 coefficient of CO₂ at in-situ temperature (K_H in mol l⁻¹ atm⁻¹) was estimated using the relationship provided in
129 (Stumm and Morgan, 1996). M_C is the molar mass of C (12 g mol⁻¹). Finally, the total CO₂ evasion was estimated by
130 summing up the product of F_D with the corresponding water surface area for all stream segments located upstream
131 of each individual sampling point.

132 **2.4 Estimation of the catchment NPP**

133 Average NPP in the catchment areas of the study sites were obtained from a global data set derived from moderate
134 resolution imaging spectroradiometer (MODIS) observations of the earth observing system (EOS) satellites, which
135 is available for the time period 2000 to 2013 with a spatial resolution of 30 arc seconds (~ 1 km²) (Zhao et al., 2005).
136 In this data set, NPP was estimated based on remote sensing observations of spectral reflectance, land cover and
137 surface meteorology as described in detail by Running et al. (2004). We used mean NPP data (2000-2013) averaged
138 over the catchment areas of the individual sampling sites.

139 **2.5 Statistical analysis**

140 Linear regressions (F-test) were used to analyze the data. Group differences or correlations with $p < 0.05$ were
141 considered statistically significant. For the regression of total aquatic C export rate and annual catchment NPP, data
142 were log-transformed to correct for normal distribution. All statistical analyses were performed with R (R
143 Development Core Team, 2011).

144 **3 Results**

145 **3.1 Catchment characteristics and aquatic C load**

146 The size of the analyzed catchment areas varied over three orders of magnitude (0.8 to 889 km²) and the mean size
147 increased from 9 km² for 1st order streams to 243 km² for streams of the order 4 (Table 1). Mean discharge and
148 catchment area were linearly correlated ($r^2=0.74$, $p < 0.001$). The runoff depth, i.e. the stream discharge divided by
149 the catchment area, was relatively constant across stream orders with a mean value of 0.28 m y⁻¹, corresponding to
150 35 % of the annual mean precipitation rate in the study area. The mean discharge increased more than 30-fold from
151 0.06 to 2.2 m³ s⁻¹ for 1st to 4th order streams, respectively. Similarly, the estimated water surface area increased with
152 increasing stream order from 0.24 to 0.42 % of the corresponding catchment size (Table 1).

153 Individual estimates of the CO₂ partial pressure at the sampling sites varied between 145 and 7759 ppm. Only 1 %
154 of the $p\text{CO}_2$ values were below the mean atmospheric value (390 ppm), indicating that the majority of the stream
155 network was a source of atmospheric CO₂ at all seasons. The $p\text{CO}_2$ was higher in summer (mean±sd: 2780±2098
156 ppm) and autumn (mean±sd: 2848±2019 ppm) than in winter (mean±sd: 2287±1716 ppm) and spring (mean±sd:
157 2172±2343 ppm). The total mean value of $p\text{CO}_2$ was 2083 ppm and $p\text{CO}_2$ and DIC did not differ significantly

158 among the different stream orders ($p\text{CO}_2$: $p=0.35$; DIC: $p=0.56$). On average, DIC in the stream water was
159 composed of 91.2 % bicarbonate, 0.4 % carbonate and 8.4 % CO_2 .

160

161 The few available samples of DOC and TOC indicate that the organic C concentration was about one order of
162 magnitude smaller than the inorganic C concentration (Table 1). There were no pronounced regional or temporal
163 differences of organic carbon. Only a small fraction of TOC was in particulate form (on average 8.6 %) and TOC
164 was linearly related to DIC, indicating that the organic load made up only 4 % of the total carbon load at the
165 sampling sites (Fig. 2). The data are provided as supplementary material.

166 3.2 Catchment NPP and C budget

167 NPP increased linearly with catchment size ($r^2=0.98$, $p<0.001$), but the specific NPP, i.e. the total NPP within a
168 catchment divided by catchment area, did not differ significantly ($p=0.24$) among catchments of different stream
169 orders. The smallest mean value and the largest variability of specific NPP (mean \pm sd: 466 ± 127 g C m^{-2} yr^{-1} , range:
170 106 to 661 g C m^{-2} yr^{-1}) was observed among the small catchments of 1st order streams, while the variability was
171 consistently smaller for higher stream orders (Table 2). The total average of terrestrial NPP in the study area was
172 515 ± 79 g C m^{-2} yr^{-1} (mean \pm sd).

173 In a simplified catchment-scale C balance, we consider the sum of the DIC discharge (DIC concentration multiplied
174 by discharge) measured at each sampling site and the total CO_2 evasion from the upstream located stream network
175 as the total amount of C that is exported from the catchment area through the aquatic conduit. The total evasion was
176 estimated by interpolation with stream-order specific $p\text{CO}_2$ values assigned to the complete stream network. Given
177 the small number of available measurements, we neglect the fraction of organic C which is exported with stream
178 discharge. As demonstrated above, TOC load is small in comparison to the DIC load (Fig. 2), resulting in a
179 comparably small (< 4 %) error.

180 The resulting CO_2 evasion rates decreased slightly, but not significantly ($p=0.26$) for increasing stream orders with a
181 total mean evasion rate of 2032 g C m^{-2} yr^{-1} (expressed as per unit water surface area) (Table 2). The total aquatic
182 evasion rate within catchments normalized by the size of the catchment increased significantly with stream order
183 with a mean value of 6.6 g C m^{-2} yr^{-1} . (Table 2).

184 The total aquatic C export rate, i.e. the sum of evasion and DIC discharge, was strongly correlated with annual mean
185 NPP averaged over the corresponding catchment area. Linear regression of the log-transformed data results in a
186 power-law exponent of 1.06, indicating a nearly linear relationship (Fig. 3). As small streams of low stream order
187 can be directly influenced by local peculiarities, the relationship is more variable for streams of Strahler order 1 and
188 2, while larger streams represent more average conditions over larger spatial scales with less variability. Most of the
189 correlation between the total aquatic C export rate and the annual mean NPP, however, can be attributed to their
190 common linear scale-dependence.

191

192 After normalization with catchment area, the total aquatic C export rate increased slightly with stream order (Fig.
193 4a). Also the ratio of the carbon exported through the aquatic network (i.e. the sum of evasion and discharge) to the
194 terrestrial NPP. Also the fraction of NPP which was exported through the aquatic network, i.e. the sum of evasion
195 and discharge, increased slightly, though not significantly ($p=0.32$), from 2.18 % for first-order stream to 2.72 % for
196 stream order 4 (Fig. 4b). This increase was related to increasing rates of CO₂ evasion in streams of higher order and
197 the contribution of evasion to the total C export rate increased from 39 to 53 % (Fig. 4c). The increasing evasion is
198 mainly caused by the increasing fractional water surface area for increasing stream orders (Table 1), because the
199 CO₂ fluxes per water surface showed a rather opposing trend with decreasing fluxes for increasing stream orders
200 (Table 2). On average 1.31 % of the catchment NPP are emitted as CO₂ from the stream network and 1.49 % are
201 discharged downstream (Table 2).

203 No regional (large-scale) pattern or gradients were observed in the spatial variation of catchment-scale NPP and
204 aquatic C export (Fig. 5).

205 **4 Discussion**

206 **4.1 Uncertainty analysis**

207 Our estimates are subject to a number of uncertainties associated with sampling and interpolation and systematic
208 errors including the neglect of carbon burial in sediments, carbon export and evasion as methane and unresolved
209 spatial and temporal variability.

210 According to Abril et al. (2015), high uncertainties of pCO₂ estimates from pH and alkalinity measurements occur at
211 pH values <7. In our study, only 7 % of the pH values were <7. For pH>7 the median and mean relative errors are
212 1% and 15%, respectively (Abril et al., 2015). Raymond et al. (2013) estimated uncertainties from comparisons of
213 estimates obtained using approaches comparable to the present study with direct measurements of CO₂
214 concentration on streams. For a density of sampling locations of 0.02 sites per km² (corresponding to this study)
215 they derived an uncertainty of 30 %. Similarly, Butman and Raymond (2011) estimated uncertainties of overall flux
216 estimates of 33 %, based on Monte Carlo simulation of similar data for hydrographic units in the United States.

217 However, we expect that these unbiased, i.e. randomly distributed, uncertainties did not affect the general results of
218 our model.

219 While the riverine carbon concentrations were obtained from measurements that covered a time period from 1977 to
220 2011, the NPP data were available for the time period from 2000 to 2013. In boreal and subtropical rivers a decadal
221 increasing DIC export due to the climate change and anthropogenic activities has been observed (Walvoord and
222 Striegl, 2007; Raymond et al., 2008), therefore the different time periods covered by the two data sets might pose a
223 problem. Comparisons of DIC measurements in the study area between 1977-1999 and 2000-2011 however did not

224 show significant changes. Furthermore, the sampling frequency for DIC increased so that the majority of DIC
225 measurements originated from the same time period as the NPP data (Supplementary Material).

226 The hydraulic geometry exponents and coefficients used in this study were derived from various data sets obtained
227 in North America, not for central Europe. Unfortunately, we are not aware of a comparably extensive data set of
228 hydraulic geometry data derived for European rivers. The coefficients have been applied in global studies before,
229 e.g. Raymond et al. (2013). A comparison of hydraulic geometry coefficients derived from various data sets,
230 including data from England, Australia and New Zealand, is presented in Butman and Raymond (2011), who
231 estimated that the error associated with uncertainties of hydraulic geometry coefficients is rather small, compared to
232 uncertainties derived for C-fluxes.

233 Carbon burial in sediments was neglected in this study but can make a significant contribution to catchment-scale C
234 balances. Estimates vary between 22 % at a global scale (Aufdenkampe et al., 2011), 14 % for the Conterminous
235 U.S. (Butman et al., 2015) and 39% for the Yellow River network (Ran et al., 2015). However, C storage in aquatic
236 systems occurs mainly in lakes and reservoirs, which are virtually absent in the study area. Therefore we consider
237 the bias caused by neglecting storage to be small in comparison to remaining uncertainties (30%).

238 Similarly, the transport of carbon as methane was neglected because measurements of methane concentration or
239 fluxes were not available for the study area. According to a recent meta-analysis, the dissolved methane
240 concentration in headwater streams varies mainly between 0.1 and 1 $\mu\text{mol L}^{-1}$, with streams in temperate forests
241 being at the lower end (Stanley et al., 2016). As the methane makes up only a small fraction of total carbon in
242 comparison to the mean DIC concentration in the present study (500 $\mu\text{mol L}^{-1}$), it can be assumed that methane
243 makes a rather small contribution to the catchment scale carbon balance.

244 Since no time-resolved discharge data were available for the sampling sites we cannot account for extreme events.
245 Moreover, no information were available if the governmental monitoring included sampling during floods. Given
246 the stochastic nature and short duration, we expect that such samples are at least underrepresented. Since it has been
247 observed that high-discharge events can make a disproportionally high contribution to annual mean carbon export
248 from catchments, we consider our estimates as a lower bound.

249 **4. 2. An average study region**

250 The average carbon fluxes in the catchments of the study area resemble global and large-scale zonal mean estimates
251 in many aspects. The mean atmospheric flux of CO_2 from the stream network of $2031 \pm 1527 \text{ g C m}^{-2} \text{ yr}^{-1}$ is in close
252 agreement with bulk estimates for streams and rivers in the temperate zone of 2630 (Aufdenkampe et al., 2011) and
253 $2370 \text{ g C m}^{-2} \text{ yr}^{-1}$ (Butman and Raymond, 2011). The fractional surface coverage of streams and rivers (0.42 % for
254 stream order 4) corresponds to the global average of 0.47 % (Raymond et al., 2013) and also mean terrestrial NPP in
255 the catchments ($515 \text{ g C m}^{-2} \text{ yr}^{-1}$) was in close correspondence to recent global mean estimates ($495 \text{ g C m}^{-2} \text{ yr}^{-1}$
256 (Zhao et al., 2005)).

257 | By combining CO_2 evasion and downstream C-export by stream discharge, we estimated that $13.9 \text{ g C m}^{-2} \text{ yr}^{-1}$,
258 | corresponding to 2.7 % of terrestrial NPP, ~~2.7 % of terrestrial NPP ($13.9 \text{ g C m}^{-2} \text{ yr}^{-1}$)~~ are exported from the

259 catchments by streams and rivers, in which both evasion and discharge contributed equally to this flux. Also these
260 findings are in close agreement with global and continental scale estimates, of 16 and 13.5 g C m⁻² yr⁻¹, respectively
261 (Table 3).

262 **4.3. Aquatic C export across spatial scales**

263 Though not exhaustive, Table 3 provides data from a large share of existing studies relating the aquatic C export to
264 terrestrial production in the corresponding catchments which cover a broad range of spatial scales and different
265 landscapes. Except for the tropical forest of the Amazon basin, the aquatic carbon export normalized to catchment
266 area estimated for temperate streams in our study, is surprisingly similar to those estimated at comparable and at
267 larger spatial scale. In the Amazon, the fraction of terrestrial production that is exported by the fluvial network is
268 more than twofold higher (nearly 7 % of NPP (Richey et al., 2002)). However, that a large fraction of the regional
269 NPP in the Amazon is supported by aquatic primary production by macrophytes and carbon export is predominantly
270 controlled by wetland connectivity, with wetlands covering up to 14 % of the land surface area (Abril et al., 2013).
271 An additional peculiarity of the Amazon is, that in contrast to the remaining systems, the vast majority (87 %) of the
272 total C export is governed by CO₂ evasion (Table 3), whereas lateral export constitutes a much smaller component.
273 An exceptionally low fraction of NPP that is exported from aquatic systems at larger scale was estimated for the
274 English Lake District (1.6 % (Maberly et al., 2013)), though only CO₂ evasion from lake surfaces was considered,
275 i.e. downstream discharge by rivers was ignored. Their estimate agrees reasonably well with the fraction of
276 catchment NPP that was emitted to the atmosphere from the stream network in the present study (1.3 %). If a similar
277 share of catchment NPP was exported with river discharge also in the Lake District, the average mass of C exported
278 from the aquatic systems per unit catchment area would be in close agreement with our and other larger-scale
279 estimates (Table 3).

280 In more detailed studies at smaller scales and for individual catchments, aquatic C export was exclusively related to
281 net ecosystem exchange (NEE) measured by eddy covariance. Here the estimated fractions of aquatic export range
282 between 2 % of NEE in a temperate forest catchment (only discharge, evasion not considered, (Shibata et al., 2005))
283 and 160 % of NEE in a boreal peatland catchment (Billett et al., 2004). Analysis of inter-annual variations of stream
284 export from a small peatland catchment in Sweden (Leach et al., 2016) resulted in estimates of C export by the
285 fluvial network between 5.9 and 18.1 g C m⁻² yr⁻¹ over 12 years. The total mean value of 12.2 g C m⁻² yr⁻¹, however,
286 is in close agreement with the present and other larger-scale estimates (Table 3). In contrast to the present study, C
287 export from the peatland catchments were dominated by stream discharge of dissolved organic carbon.

288 **4.4 Controlling factors for aquatic C export**

289 We found a significant linear relationship between total catchment NPP and the C export from the catchment in the
290 stream network across four Strahler orders. The relationship was mainly caused by a strong correlation between
291 catchment size and water surface area. As expected for temperate zones, large streams and rivers with large surface
292 area have larger catchments. A study analyzing aquatic carbon fluxes for 18 hydrological units in the conterminous

293 U.S. (Butman et al., 2015) observed a significant correlation between catchment-specific aquatic C yield and
294 specific catchment NEP, which in turn was linearly correlated to NPP. We did not observe such correlation at
295 smaller scale, which could be related to the rather narrow range of variability in NPP among the considered
296 catchments. Nevertheless, the linear correlation observed by (Butman et al., 2015) indicates that a constant fraction
297 of terrestrial NPP is exported by aquatic systems if averaged over larger spatial scales.

298 The relatively narrow range of variability of C export per catchment area (between 9 and 18 g C m⁻² yr⁻¹, with the
299 two exceptions discussed above) in different landscapes (Table 3) is rather surprising. Although this range of
300 variation is most likely within the uncertainty of the various estimates, the variability across different landscapes is
301 certainly small in comparison to the order of magnitude differences in potential controlling factors like catchment
302 NPP, fractional water coverage as well as size and climatic zone of the study area. In lake-rich regions, evasion from
303 inland waters was observed to be dominated by lakes (Buffam et al., 2011;Jonsson et al., 2007), which cover up to
304 13 % of the surface area of these regions. In the present as well as in other studies on catchments where lakes are
305 virtually absent (Wallin et al., 2013) and the fractional water coverage was smaller than 0.5 % of the terrestrial
306 surface area, an almost identical catchment-specific C export and evasion rate has been observed (Table 3). CO₂
307 emissions from water surfaces depend on the partial pressure of CO₂ in water and are therefore related to DIC,
308 which was the dominant form of dissolved C in the present study. Studies in the boreal zone, where dissolved C in
309 the aquatic systems is mainly in the form of DOC, however, found comparable catchment-specific C export and
310 evasion rates ((Leach et al., 2016;Jonsson et al., 2007;Wallin et al., 2013), cf. Table 3). The difference in the
311 speciation of the exported C indicates that a larger fraction of the terrestrial NPP is respired by heterotrophic
312 respiration in soils and exported to the stream network as DIC in the present study, in contrast to export as DOC and
313 predominantly aquatic respiration. Observations and modeling of terrestrial-aquatic C fluxes across the U.S.
314 suggested a transition of the source of aquatic CO₂ from direct terrestrial input to aquatic CO₂ production by
315 degradation of terrestrial organic carbon with increasing stream size (Hotchkiss et al., 2015). Such transition was not
316 observed in the present study, where organic carbon made a small contribution to the fluvial carbon load across all
317 investigated stream orders. In addition to soil respiration, mineral weathering also contributes to DIC in stream
318 water. The relative importance of soil respiration and weathering varies depending on geology and the presence of
319 wetlands in the area (Hotchkiss et al., 2015;Lauerwald et al., 2013;Jones et al., 2003). In the present study, 16 % of
320 the catchment areas contained carbonate bedrock. The DIC concentration in the water increased with the proportion
321 of carbonate containing bedrock in the catchment ($R^2=0.33, p<0.001$).

322 Despite the small number of observations in the meta-analysis, the narrow range of variability of C export per
323 catchment area may indicate that neither water surface area nor the location of mineralization of terrestrial derived C
324 (soil respiration and export of DIC versus export of DOC and mineralization in the aquatic environment), are
325 important drivers for the total C export from catchments by inland waters at larger spatial scales. This rather
326 unexpected finding deserves further attention, as it suggests that other, currently poorly explored, processes control
327 the aquatic-terrestrial coupling and the role of inland waters in regional C cycling. Given the significant contribution
328 of inland waters to regional and global scale greenhouse gas emissions, the mechanistic understanding of these

329 processes is urgently required to assess their vulnerability to ongoing climatic and land use changes, as well to the
330 extensive anthropogenic influences on freshwater ecosystems. Recent developments of process-based models, which
331 are capable of resolving the boundless biogeochemical cycle in the terrestrial–aquatic continuum from catchment to
332 continental scales (Nakayama, 2016), are certainly an important tool for these future studies.

333

334 **5 Conclusion:**

335 Our analysis of the carbon budget in a temperate stream network on regional scale revealed a relationship of aquatic
336 carbon export and terrestrial NPP. On average $13.9 \text{ g C m}^{-2} \text{ yr}^{-1}$, corresponding to 2.7 % of the terrestrial NPP, were
337 exported from the catchments by rivers and stream with CO_2 evasion and downstream transport contributing equally
338 to the export. A comparison of our regional scale study with other studies from different scales and landscapes
339 showed a relatively narrow range of variability of carbon export per catchment area. Future research is needed to
340 understand the processes that control the aquatic-terrestrial coupling and the role of inland waters in regional carbon
341 cycling.

342

343

344

345

346

347 **Acknowledgments**

348 This study was financially supported by the German Research Foundation (grant no. LO 1150/9-1). We thank
349 Miriam Tenhaken for contributing to a preliminary analysis. All raw data for this paper is properly cited and referred
350 to in the reference list. The processed data, which were used to generate the figures and tables, are available upon
351 request through the corresponding author.

- 353 Abril, G., Martinez, J.-M., Artigas, L. F., Moreira-Turcq, P., Benedetti, M. F., Vidal, L.,
354 Meziane, T., Kim, J.-H., Bernardes, M. C., Savoye, N., Deborde, J., Souza, E. L., Alberic, P.,
355 Landim de Souza, M. F., and Roland, F.: Amazon River carbon dioxide outgassing fuelled by
356 wetlands, *Nature*, 505, 395-398, 10.1038/nature12797, 2013.
- 357 Abril, G., Bouillon, S., Darchambeau, F., Teodoru, C. R., Marwick, T. R., Tamooh, F., Omengo,
358 F. O., Geeraert, N., Deirmendjian, L., and Polsemaere, P.: Technical Note: Large overestimation
359 of pCO₂ calculated from pH and alkalinity in acidic, organic-rich freshwaters, *Biogeosciences*,
360 12, 67, 2015.
- 361 Aufdenkampe, A. K., Mayorga, E., Raymond, P. A., Melack, J. M., Doney, S. C., Alin, S. R.,
362 Aalto, R. E., and Yoo, K.: Riverine coupling of biogeochemical cycles between land, oceans, and
363 atmosphere, *Front. Ecol. Environ.*, 9, 53-60, 10.1890/100014, 2011.
- 364 Barros, N., Cole, J. J., Tranvik, L. J., Prairie, Y. T., Bastviken, D., Huszar, V. L. M., del Giorgio,
365 P., and Roland, F.: Carbon emission from hydroelectric reservoirs linked to reservoir age and
366 latitude, *Nature Geosci.*, 4, 593-596, 10.1038/ngeo1211, 2011.
- 367 Battin, T. J., Luysaert, S., Kaplan, L. A., Aufdenkampe, A. K., Richter, A., and Tranvik, L. J.:
368 The boundless carbon cycle, *Nature Geosci.*, 2, 598-600, 10.1038/ngeo618, 2009.
- 369 Billett, M. F., Palmer, S. M., Hope, D., Deacon, C., Storeton-West, R., Hargreaves, K. J.,
370 Flechard, C., and Fowler, D.: Linking land-atmosphere-stream carbon fluxes in a lowland
371 peatland system, *Global Biogeochem. Cycles*, 18, 10.1029/2003GB002058, 2004.
- 372 Buffam, I., Turner, M. G., Desai, A. R., Hanson, P. C., Rusak, J. A., Lottig, N. R., Stanley, E. H.,
373 and Carpenter, S. R.: Integrating aquatic and terrestrial components to construct a complete
374 carbon budget for a north temperate lake district, *Global Change Biol.*, 17, 1193-1211,
375 10.1111/j.1365-2486.2010.02313.x, 2011.
- 376 Butman, D., and Raymond, P. A.: Significant efflux of carbon dioxide from streams and rivers in
377 the United States, *Nature Geosci.*, 4, 839-842, 2011.
- 378 Butman, D., Stackpoole, S., Stets, E., McDonald, C. P., Clow, D. W., and Striegl, R. G.: Aquatic
379 carbon cycling in the conterminous United States and implications for terrestrial carbon
380 accounting, *Proceedings of the National Academy of Sciences*, 10.1073/pnas.1512651112, 2015.
- 381 Christensen, T. R., Johansson, T., Olsrud, M., Ström, L., Lindroth, A., Mastepanov, M., Malmer,
382 N., Friborg, T., Crill, P., and Callaghan, T. V.: A catchment-scale carbon and greenhouse gas
383 budget of a subarctic landscape, *Philosophical Transactions of the Royal Society of London A:
384 Mathematical, Physical and Engineering Sciences*, 365, 1643-1656, 10.1098/rsta.2007.2035,
385 2007.
- 386 Cole, J. J., Prairie, Y. T., Caraco, N. F., McDowell, W. H., Tranvik, L. J., Striegl, R. G., Duarte,
387 C. M., Kortelainen, P., Downing, J. A., Middelburg, J. J., and Melack, J.: Plumbing the global
388 carbon cycle: Integrating inland waters into the terrestrial carbon budget, *Ecosystems*, 10, 171-
389 184, 10.1007/s10021-006-9013-8, 2007.
- 390 DIN EN ISO 9963-1:1996-02: Wasserbeschaffenheit - Bestimmung der Alkalinität - Teil 1:
391 Bestimmung der gesamten und der zusammengesetzten Alkalinität (ISO 9963-1:1994); German
392 version EN ISO 9963-1:1995,
- 393 DIN EN ISO 9963-2:1996-02: Wasserbeschaffenheit - Bestimmung der Alkalinität - Teil 2:
394 Bestimmung der Carbonatalkalinität (ISO 9963-2:1994); German version EN ISO 9963-2:1995,

395 DIN EN ISO 10523:2012-04: Wasserbeschaffenheit - Bestimmung des pH-Werts (ISO
396 10523:2008); German version EN ISO 10523:2012.

397 EEA: Corine Land Cover 2006 seamless vector data, European Environment Agency, 2006.

398 Hotchkiss, E. R., Hall Jr, R. O., Sponseller, R. A., Butman, D., Klaminder, J., Laudon, H.,
399 Rosvall, M., and Karlsson, J.: Sources of and processes controlling CO₂ emissions change with
400 the size of streams and rivers, *Nature Geosci.*, 8, 696-699, 10.1038/ngeo2507, 2015.

401 Jones, J. B., Stanley, E. H., and Mulholland, P. J.: Long-term decline in carbon dioxide
402 supersaturation in rivers across the contiguous United States, *Geophysical Research Letters*, 30,
403 2003.

404 Jonsson, A., Algesten, G., Bergström, A. K., Bishop, K., Sobek, S., Tranvik, L. J., and Jansson,
405 M.: Integrating aquatic carbon fluxes in a boreal catchment carbon budget, *J. Hydrol.*, 334, 141-
406 150, 10.1016/j.jhydrol.2006.10.003, 2007.

407 Lauerwald, R., Hartmann, J., Moosdorf, N., Kempe, S., and Raymond, P. A.: What controls the
408 spatial patterns of the riverine carbonate system?—A case study for North America, *Chemical
409 geology*, 337, 114-127, 2013.

410 Lauerwald, R., Laruelle, G. G., Hartmann, J., Ciais, P., and Regnier, P. A.: Spatial patterns in
411 CO₂ evasion from the global river network, *Global Biogeochemical Cycles*, 29, 534-554, 2015.

412 Leach, J. A., Larsson, A., Wallin, M. B., Nilsson, M. B., and Laudon, H.: Twelve year
413 interannual and seasonal variability of stream carbon export from a boreal peatland catchment, *J.
414 Geophys. Res.-Biogeo.*, 121, 1851–1866, 10.1002/2016JG003357, 2016.

415 Leopold, L. B., and Maddock Jr, T.: The hydraulic geometry of stream channels and some
416 physiographic implications2330-7102, 1953.

417 LVermGeoRP: Vermessungs- und Katasterverwaltung Rheinland-Pfalz, Landesamt für
418 Vermessung und Geobasisinformation Rheinland-Pfalz, 2012.

419 Maberly, S. C., Barker, P. A., Stott, A. W., and De Ville, M. M.: Catchment productivity
420 controls CO₂ emissions from lakes, *Nat. Clim. Chang.*, 3, 391-394, 10.1038/nclimate1748, 2013.

421 MULEWF: GeoPortal Wasser, Ministerium für Umwelt, Landwirtschaft, Ernährung, Weinbau
422 und Forsten Rheinland-Pfalz, 2013.

423 MULEWF: Wasserwirtschaftsverwaltung Rheinland-Pfalz, Ministerium für Umwelt,
424 Landwirtschaft, Ernährung, Weinbau und Forsten Rheinland-Pfalz, 2015.

425 Nakayama, T.: New perspective for eco-hydrology model to constrain missing role of inland
426 waters on boundless biogeochemical cycle in terrestrial–aquatic continuum, *Ecology &
427 Hydrobiology*, 16, 138-148, 10.1016/j.ecohyd.2016.07.002, 2016.

428 Parkhurst, D. L., and Appelo, C.: User's guide to PHREEQC (Version 2): A computer program
429 for speciation, batch-reaction, one-dimensional transport, and inverse geochemical calculations,
430 1999.

431 R Development Core Team: R: A language and environment for statistical computing. R
432 Foundation for Statistical Computing, Vienna, Austria, 2011.

433 Ran, L., Lu, X. X., Yang, H., Li, L., Yu, R., Sun, H., and Han, J.: CO₂ outgassing from the
434 Yellow River network and its implications for riverine carbon cycle, *J. Geophys. Res.-Biogeo.*,
435 120, 1334-1347, 10.1002/2015JG002982, 2015.

436 Randerson, J. T., Chapin, F. S., Harden, J. W., Neff, J. C., and Harmon, M. E.: Net ecosystem
437 production: a comprehensive measure of net carbon accumulation by ecosystems, *Ecol.
438 Applications*, 12, 937-947, 10.1890/1051-0761(2002)012[0937:NEPACM]2.0.CO;2, 2002.

439 Raymond, P. A., Oh, N.-H., Turner, R. E., and Broussard, W.: Anthropogenically enhanced
440 fluxes of water and carbon from the Mississippi River, *Nature*, 451, 449-452, 2008.

441 Raymond, P. A., Zappa, C. J., Butman, D., Bott, T. L., Potter, J., Mulholland, P., Laursen, A. E.,
442 McDowell, W. H., and Newbold, D.: Scaling the gas transfer velocity and hydraulic geometry in
443 streams and small rivers, *Limnology and Oceanography: Fluids and Environments*, 2, 41-53,
444 2012.

445 Raymond, P. A., Hartmann, J., Lauerwald, R., Sobek, S., McDonald, C., Hoover, M., Butman,
446 D., Striegl, R., Mayorga, E., Humborg, C., Kortelainen, P., Durr, H., Meybeck, M., Ciais, P., and
447 Guth, P.: Global carbon dioxide emissions from inland waters, *Nature*, 503, 355-359,
448 10.1038/nature12760, 2013.

449 Richey, J. E., Melack, J. M., Aufdenkampe, A. K., Ballester, V. M., and Hess, L. L.: Outgassing
450 from Amazonian rivers and wetlands as a large tropical source of atmospheric CO₂, *Nature*, 416,
451 617-620, 10.1038/416617a, 2002.

452 Running, S. W., Nemani, R. R., Heinsch, F. A., Zhao, M., Reeves, M., and Hashimoto, H.: A
453 Continuous Satellite-Derived Measure of Global Terrestrial Primary Production, *Bioscience*, 54,
454 547-560, 10.1641/0006-3568(2004)054[0547:acsmog]2.0.co;2, 2004.

455 Sabine, C. L., Heimann, M., Artaxo, P., Bakker, D. C., Chen, C.-T. A., Field, C. B., Gruber, N.,
456 Le Quéré, C., Prinn, R. G., and Richey, J. E.: Current status and past trends of the global carbon
457 cycle, in: *The Global Carbon Cycle*, 2nd ed., edited by: Field, C. B., and Raupach, M. R.,
458 Scientific Committee on Problems of the Environment (SCOPE) Series, Island Press, 17-44,
459 2004.

460 Shibata, H., Hiura, T., Tanaka, Y., Takagi, K., and Koike, T.: Carbon cycling and budget in a
461 forested basin of southwestern Hokkaido, northern Japan, *Ecological Research*, 20, 325-331,
462 10.1007/s11284-005-0048-7, 2005.

463 Stanley, E. H., Casson, N. J., Christel, S. T., Crawford, J. T., Loken, L. C., and Oliver, S. K.: *The
464 ecology of methane in streams and rivers: patterns, controls, and global significance*, Ecological
465 Monographs, 2016.

466 Statistisches Landesamt Rheinland-Pfalz: *Statistisches Jahrbuch 2014*, 2014.

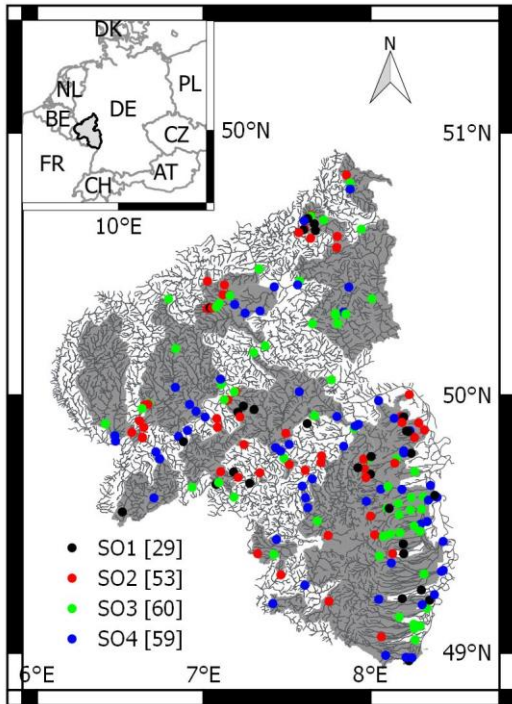
467 Strahler, A. N.: Quantitative analysis of watershed geomorphology, *Eos, Transactions American
468 Geophysical Union*, 38, 913-920, 1957.

469 Stumm, W., and Morgan, J. J.: *Aquatic chemistry: chemical equilibria and rates in natural
470 waters*, Wiley, 1996.

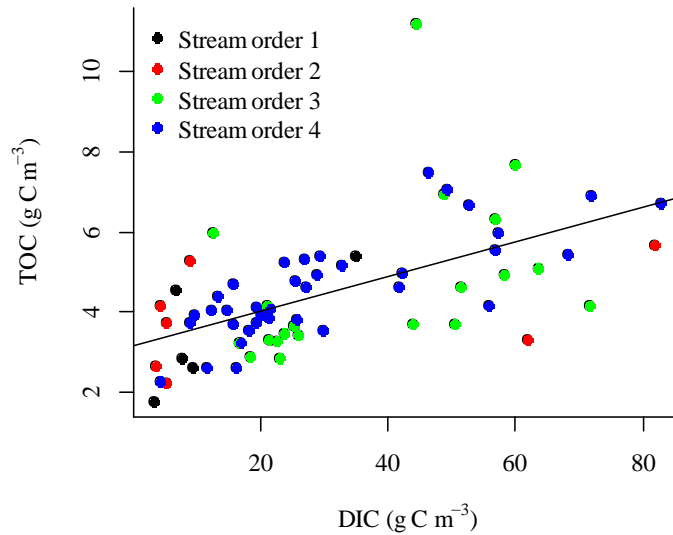
471 Tranvik, L. J., Downing, J. A., Cotner, J. B., Loiselle, S. A., Striegl, R. G., Ballatore, T. J.,
472 Dillon, P., Finlay, K., Fortino, K., Knoll, L. B., Kortelainen, P. L., Kutser, T., Larsen, S.,
473 Laurion, I., Leech, D. M., McCallister, S. L., McKnight, D. M., Melack, J. M., Overholt, E.,
474 Porter, J. A., Prairie, Y., Renwick, W. H., Roland, F., Sherman, B. S., Schindler, D. W., Sobek,
475 S., Tremblay, A., Vanni, M. J., Verschoor, A. M., von Wachenfeldt, E., and Weyhenmeyer, G.
476 A.: Lakes and reservoirs as regulators of carbon cycling and climate, *Limnol. Oceanogr.*, 54,
477 2298-2314, 10.4319/lo.2009.54.6_part_2.2298, 2009.

478 Wallin, M. B., Grabs, T., Buffam, I., Laudon, H., Ågren, A., Öquist, M. G., and Bishop, K.:
479 Evasion of CO₂ from streams – The dominant component of the carbon export through the
480 aquatic conduit in a boreal landscape, *Global Change Biol.*, 19, 785-797, 10.1111/gcb.12083,
481 2013.

482 Walvoord, M. A., and Striegl, R. G.: Increased groundwater to stream discharge from permafrost
483 thawing in the Yukon River basin: Potential impacts on lateral export of carbon and nitrogen,
484 Geophysical Research Letters, 34, 2007.
485 Zhang, W., and Montgomery, D. R.: Digital elevation model grid size, landscape representation,
486 and hydrologic simulations, Water Resour. Res., 30, 1019-1028, 10.1029/93WR03553, 1994.
487 Zhao, M., Heinsch, F. A., Nemani, R. R., and Running, S. W.: Improvements of the MODIS
488 terrestrial gross and net primary production global data set, Remote Sensing of Environment, 95,
489 164-176, 10.1016/j.rse.2004.12.011, 2005.



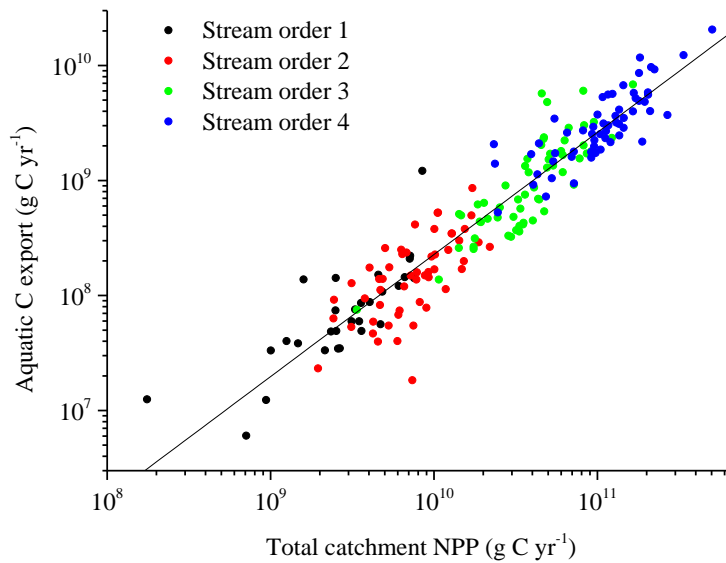
490
491 **Fig. 1:** Map of the stream network (black lines) within the state borders of Rhineland Palatinate in southwest Germany.
492 The inset map in the upper left corner indicates the location of the study region in central Europe. Filled circles mark the
493 position of sampling sites with color indicating stream order (SO1 – SO4; the numbers in brackets in the legend are the
494 respective number of sampling sites). The catchment areas of the sampling sites are marked in grey color.
495



496

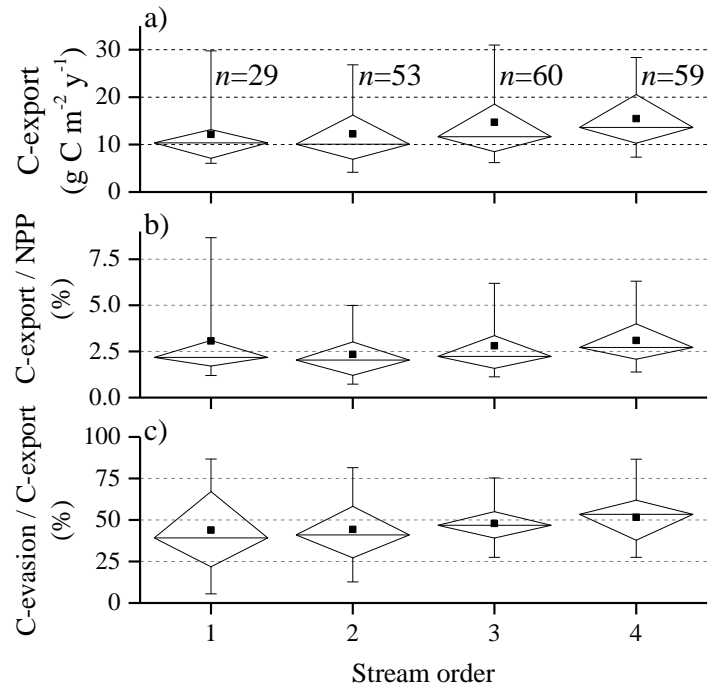
497 **Fig. 2: TOC concentration versus DIC concentration. Different colors indicate sampling sites from different stream**
 498 **orders. The solid line shows the fitted linear regression model with $TOC=0.04 \cdot DIC$ ($r^2=0.33, p<0.001$).**

499



500

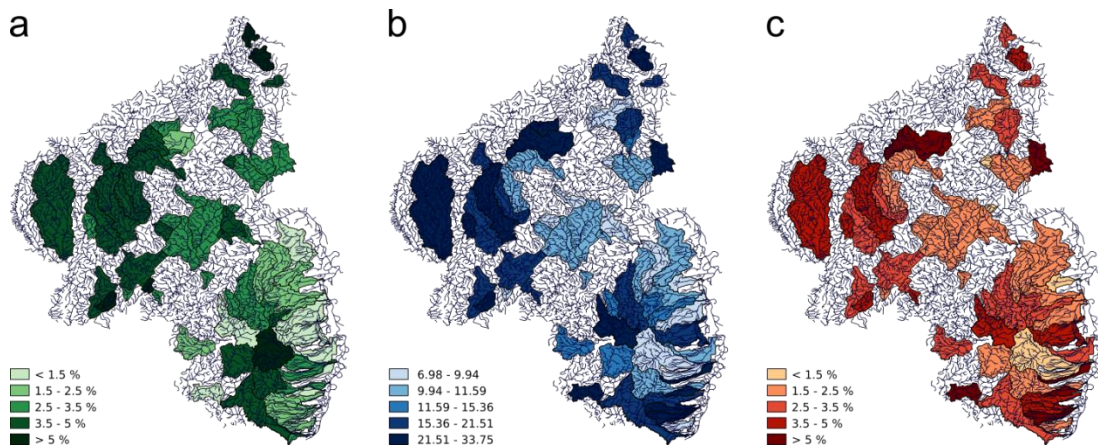
501 **Fig. 3: Annual rate of C export through the stream network versus terrestrial NPP in the catchment area. Different colors**
 502 **indicate sampling sites from different stream orders. The solid line shows the fitted linear regression model for the log-**
 503 **transformed data with $C_export=0.005 \cdot NPP^{1.06}$ ($r^2=0.89, p<0.001$).**



505

506 **Fig. 4:** a) Boxplots of C export (sum of evasion and discharge) normalized by catchment area. b) Boxplots of the ratio of
 507 the total exported C and terrestrial NPP for different stream orders. c) Boxplots of the fraction of the total exported C
 508 which is emitted to the atmosphere from the stream network for each stream order. The boxes demarcate the 25th and
 509 75th percentiles, the whiskers demarcate the 95% confidence intervals. Median and mean values are marked as
 510 horizontal lines and square symbols, respectively. The sample numbers (n) provided in a) apply to all panels.

511



512

513 **Fig. 5:** Map of 3rd and 4th order catchments showing a) Mean NPP ($\text{g C m}^{-2} \text{yr}^{-1}$), b) aquatic export ($\text{g C m}^{-2} \text{yr}^{-1}$), c) ratio
 514 aquatic export/NPP (%).

515

516 **Table 1: Major hydrological characteristics, $p\text{CO}_2$, DIC and DOC concentrations averaged over stream orders (SO) and**
 517 **for all sampling sites (total). All values are provided as mean \pm sd (standard deviation) of the annual mean observations,**
 518 **ranges are given in brackets, n is the number of observations.**

	SO 1	SO 2	SO 3	SO 4	Total
n	29	53	60	59	201
Catchment size (km^2)	9 \pm 7 (1 – 35)	16 \pm 9 (4 – 37)	87 \pm 54 (9 – 298)	243 \pm 140 (48 – 889)	103 \pm 126 (1 – 889)
Water coverage (%)	0.24 \pm 0.11 (0.05 – 0.43)	0.26 \pm 0.09 (0.1 – 0.45)	0.36 \pm 0.11 (0.09 – 0.6)	0.42 \pm 0.13 (0.18 – 0.7)	0.33 \pm 0.13 (0.05 – 0.7)
Discharge ($\text{m}^3 \text{s}^{-1}$)	0.06 \pm 0.05 (0.003 – 0.19)	0.15 \pm 0.10 (0.01 – 0.36)	0.73 \pm 0.63 (0.02 – 3.41)	2.20 \pm 1.95 (0.22 – 12.22)	0.91 \pm 1.41 (0.003 – 12.22)
Drainage rate (m y^{-1})	0.26 \pm 0.17 (0.05 – 0.67)	0.29 \pm 0.16 (0.06 – 0.66)	0.27 \pm 0.17 (0.05 – 0.74)	0.30 \pm 0.21 (0.06 – 1.20)	0.28 \pm 0.18 (0.05 – 1.20)
pH	7.58 \pm 0.61 (6.20 – 8.97)	7.70 \pm 0.46 (6.30 – 8.60)	7.81 \pm 0.37 (6.60 – 8.30)	7.75 \pm 0.29 (6.91 – 8.30)	7.73 \pm 0.42 (6.20 – 8.97)
Alkalinity (mmol L^{-1})	3.08 \pm 2.50 (0.08 – 7.58)	2.74 \pm 2.58 (0.08 – 8.55)	2.77 \pm 1.85 (0.14 – 9.88)	2.58 \pm 1.73 (0.32 – 7.22)	2.75 \pm 2.12 (0.08 – 9.88)
$p\text{CO}_2$ (ppm)	2597 \pm 1496 (145 – 6706)	1819 \pm 1095 (681 – 5338)	1992 \pm 1327 (573 – 7627)	2162 \pm 1302 (366 – 7759)	2083 \pm 1303 (145 – 7759)
DIC (g m^{-3})	38.8 \pm 30.3 (3.4 – 93.1)	34.2 \pm 31.1 (3.5 – 104.5)	34.6 \pm 22.4 (3.1 – 119.6)	32.4 \pm 21.0 (4.1 – 89.3)	34.5 \pm 25.7 (3.1 – 119.6)
DOC (g m^{-3})	3.54 \pm 1.86 (2.2 – 6.7) ($n=5$)	4.11 \pm 0.73 (3.1 – 4.8) ($n=4$)	4.17 \pm 1.08 (2.6 – 7.1) ($n=22$)	4.10 \pm 1.24 (2.0 – 7.7) ($n=33$)	4.08 \pm 1.20 (2.0 – 7.7) ($n=64$)

519

520 **Table 2: Aquatic C-fluxes and terrestrial NPP in catchments drained by streams of different stream orders (SO) and for**
 521 **all sampling sites (total). All values are mean \pm standard deviation, ranges are given in brackets. The CO_2 flux from the**
 522 **water surface (first row) is expressed per square meter water surface area, while the remaining fluxes are expressed per**
 523 **square meter catchment area.**

	SO 1	SO 2	SO 3	SO 4	Total
CO ₂ flux from water surface (g C m ⁻² yr ⁻¹)	2415±2335 (-335 – 12915)	1975±1364 (418 – 7143)	1998±1671 (704 – 11016)	1928±903 (851 – 5093)	2032±1528 (-335 – 12915)
Gas transfer velocity k ₆₀₀ (m d ⁻¹)	7.04±4.52 (2.16 – 20.57)	7.74±3.78 (2.03 – 20.50)	5.86±2.81 (2.03 – 15.55)	4.23±0.96 (2.03 – 6.50)	6.05±3.32 (2.03 – 20.57)
CO ₂ evasion per catchment area (g C m ⁻² yr ⁻¹)	5.9±6.3 (-1.0 – 30.0)	5.2±4.1 (0.7 – 19.2)	7.0±6.6 (1.6 – 43.8)	8.0±4.6 (3.0 – 23.0)	6.6±5.5 (-1.0 – 43.8)
DIC discharge per catchment area (g C m ⁻² yr ⁻¹)	6.2±4.5 (1.6 – 25.8)	7.1±6.1 (0.6 – 27.2)	7.7±5.7 (1.6 – 35.5)	7.5±4.7 (1.2 – 24.5)	7.3±5.4 (0.6 – 35.5)
Total aquatic C export per catchment area (g C m ⁻² yr ⁻¹)	12.1±6.9 (4.7 – 34.5)	12.3±6.9 (1.5 – 29.6)	14.7±10.8 (5.3 – 66.8)	15.5±6.7 (7.0 – 33.8)	13.9±8.3 (1.5 – 66.8)
NPP (g C m ⁻² yr ⁻¹)	466±127 (106 – 661)	536±66 (251 – 644)	527±57 (364 – 627)	508±69 (330 – 618)	515±79 (106 – 661)

524

525 **Table 3: Summary of estimates of aquatic C export in relation to terrestrial production in the watershed across different**
526 **spatial scales (spatial scale decreases from top to bottom). Aquatic C export is the sum of C-discharge and evasion**
527 **(numbers in parentheses also include the change in C storage in the aquatic systems by sedimentation) normalized by the**
528 **area of the terrestrial watershed. Aquatic C fate refers to the percentage of the total exported C which is emitted to the**
529 **atmosphere (evasion) and transported downstream (discharge). The missing percentage is the fraction which is stored in**
530 **the aquatic systems by sedimentation (if considered). Terrestrial production is expressed as NPP or as net ecosystem**
531 **exchange (NEE). n.c. indicates that this compartment/flux was not considered in the respective study.**

Study area (Catchment size in km ²)	Fractional water coverage (%) Rivers Lakes	Aquatic C export (g C m ⁻² yr ⁻¹)	Aquatic C fate (%): Evasion Discharge	Aquatic C export / terrestrial production (%)		Reference
				NPP	NEE	
Global (1.3x10 ⁸)	R: 0.2-0.3 L: 2.1-3.4	16 (20)	E: 44 D: 34	3.7 ¹	21-64 ²	(Aufdenkampe et al., 2011)
Conterminous U.S. (7.8x10 ⁶)	R: 0.52 L: 1.6	13.5 (18.8)	E: 58 D: 28	3.6	27 ³	(Butman et al., 2015)
Central Amazon (1.8x10 ⁶)	4-16	78138	E: 87 D: 13	6.8 ⁴	n.c.	(Richey et al., 2002)
Yellow River network (7.5x10 ⁵)	R: 0.3-0.4 L: n.c.	18.5 (30)	E: 35 D: 26	n.c.	96 (62)	(Ran et al., 2015)
North temperate	R: 0.5	11.8	E: 33	n.c.	7	(Buffam et al.,

lake district (6400)	L: 13	(16)	D: 41			2011)
Northern Sweden (peat) (3025)	R: 0.33 L: 3.5	9	E: 50 (4.5) D: 50 (4.5)	n.c.	6	(Jonsson et al., 2007)
Temperate streams (0.7- 1227)	R: 0.33 L: n.c.	13.9	E: 47 D: 53	2.7	n.c.	This study
English Lake district (1 - 360)	R: n.c. L: 2.2	5.4	E: 100 D: n.c.	1.6	n.c.	(Maberly et al., 2013)
Forested stream catchments in Sweden (0.46 - 67)	R: 0.1-0.7 L:n.c. (<0.7)	9.4	E: 53 D: 47	n.c.	8-17	(Wallin et al., 2013)
Forest catchment in Japan (9.4)	R: - L: n.c.	4	E: n.c. D: 100	n.c.	2	(Shibata et al., 2005)
Peatland catchment (3.35)	R: 0.05 L: n.c.	30.4	E: 13 D: 87	n.c.	160	(Billett et al., 2004)
Peatland catchment (2.7)	R: n.c. L: 2.2	12.2	E: - D: -	n.c.	12-50	(Leach et al., 2016)

532 ¹ For a value of 56 Pg C yr⁻¹ for global NPP (Zhao et al., 2005).

533 ² Global mean NEE was estimated as the difference of GPP and ecosystem respiration, which was assumed to be 91-
534 97 % of GPP (Randerson et al., 2002).

535 ³ This percentage refers to NEP instead of NEE.

536 ⁴ For a global mean value of NPP in tropical forests of 1148 g C m⁻² yr⁻¹ (Sabine et al., 2004).

537